JOC The Journal of Organic Chemistry

Article

pubs.acs.org/joc

Aza-Crown Macrocycles as Chiral Solvating Agents for Mandelic Acid Derivatives

Thomas P. Quinn,[†] Philip D. Atwood,[†] Joseph M. Tanski,[‡] Tyler F. Moore,[†] and J. Frantz Folmer-Andersen*,[†]

[†]Department of Chemistry, The State University of New York at New Paltz, 1 Hawk Drive, New Paltz, New York 12561, United States

[‡]Department of Chemistry, Vassar College, 124 Raymond Avenue, Box 601, Poughkeepsie, New York 12604, United States

Supporting Information

ABSTRACT: A series of new chiral macrocycles containing the *trans*-1,2-diaminocyclohexane (DACH) subunit and arene- and oligoethylene glycol-derived spacers has been prepared in enantiomerically pure form. Four of the macrocycles have been characterized by X-ray crystallography, which reveals a consistent mode of intramolecular N−H···N hydrogen bonding and conformational variations about the *N*-benzylic bonds. Most of the macrocycles were found to differentiate the enantiomers of mandelic acid (MA) by ^{1}H NMR spectroscopy in $CDCl_3$; within the series of macrocycles tested, enantiodiscrimination was promoted by (i) a *meta*-linkage geometry about the arene spacer, (ii) the presence of naphthalene- rather than phenylene-derived arene spacers, and (iii) increasing length of the oligoethylene glycol bridge. ^{1}H NMR titrations were performed with optically pure MA samples, and the data were fitted to a simultaneous 1:1 and 2:1 binding model, yielding estimates of 2:1 binding constants between some of the macrocycles and MA enantiomers. In several cases, NOESY spectra of the MA:macrocycle complexes show differential intramolecular correlations between protons adjacent to the amine and carboxylic acid groups of the macrocycles and MA enantiomers, respectively, thus demonstrating geometric differences between the diastereomeric intermolecular complexes. The three most effective macrocycles were employed as chiral solvating agents (CSAs) to determine the enantiomeric excess (ee) of 18 MA samples over a wide ee range and with very high accuracy (1% absolute error).

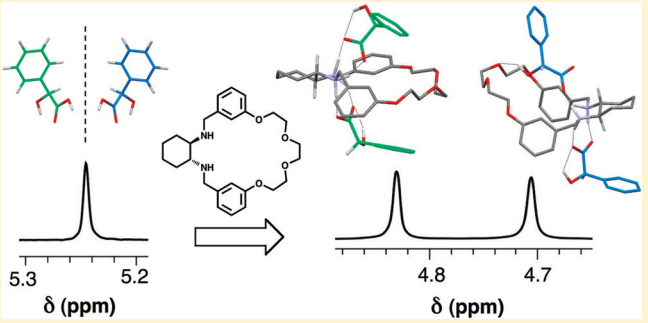

INTRODUCTION

The development of synthetic receptors that are capable of differentially binding enantiomeric substrates is an important goal,[1] relating both to the advancement of fundamental knowledge of molecular recognition phenomena[2] and to more practical applications focused on discriminating enantiomers for preparative[3] and analytical[4] purposes. Thermodynamic enantioselection is predicated on the ability of a chiral host molecule to form energetically distinct diastereomeric complexes with enantiomeric guests. Despite sustained interest in the problem since soon after the inception of modern supramolecular chemistry,[5] it remains a considerable challenge to realize binding enantioselecivities in synthetic systems that are comparable to those of protein−substrate complexes. For example, the blood coagulation protein thrombin binds small-molecule inhibitors with enantioselectivities ($K_{(R)}/K_{(S)}$) approaching 800:1 ($\Delta\Delta G_{enantio} \sim 4$ kcal mol^{-1} at 298 K),[6] whereas selectivity factors of 10 ($\Delta\Delta G_{enantio} = 1.4$ kcal mol^{-1} at 298 K) are generally considered impressive for synthetic host molecules.[2c,5e,7] Such disparities are likely related to differing degrees of substrate encapsulation and structural complementarity, and their magnitudes highlight the latent potential of supramolecular chemistry as a means of selectively addressing enantiomers.

A key analytical application that has emerged from enantioselective host−guest chemistry is the use of chiral solvating agents (CSAs) for NMR spectroscopy.[4e,8] CSAs are essentially chiral receptors that differentiate the NMR signals of enantiomeric guests upon complexation, usually allowing for the enantiomeric excess (ee) of the guest sample to be determined but also providing absolute configurations of guests in some cases. Among the most familiar CSAs are chiral lanthanide complexes[8a,b] which induce large, differential ^{1}H NMR shifts in a wide range of enantiomeric donor groups upon metal coordination. Despite the versatility of lanthanide-based CSAs, complications associated with paramagnetic line broadening at higher field strengths and difficulties in elucidating the mechanisms of chiral discrimination have encouraged the development of alternative CSAs. Unlike chiral derivatizing agents,[8a,b,9] which rely on covalent bond formation to desymmetrize enantiomers and have also been used extensively

Received: September 2, 2011
Published: October 31, 2011

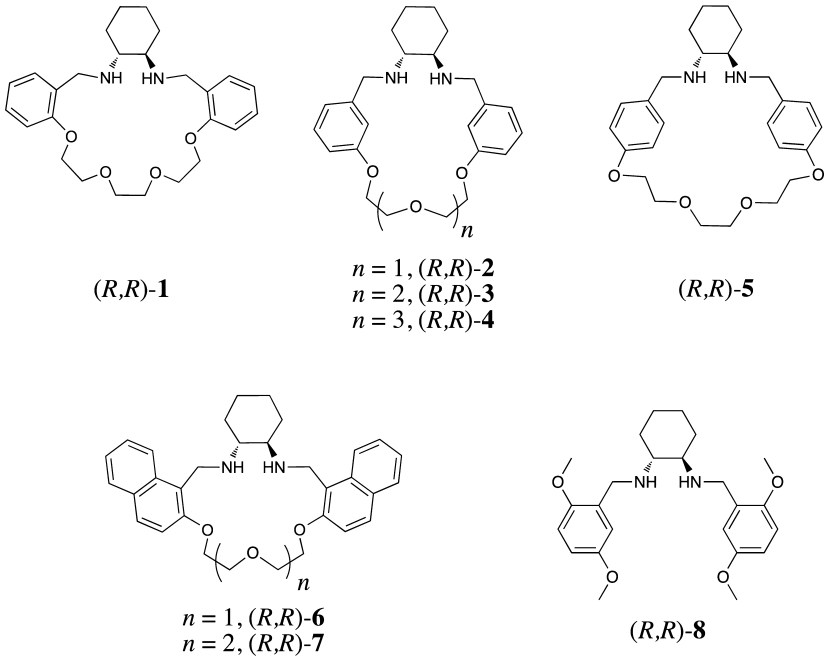

Figure 1. Structures of the receptors examined in this study.

for ee measurement by NMR, CSAs do not require chemical modification of the sample, thus obviating derivatization chemistry and facilitating sample recovery. CSAs also offer a significant advantage over chromatographic methods of ee analysis, in that they avoid the inherently laborious process of physically separating enantiomers. In light of these features, the development of synthetic receptors as CSAs represents a promising approach toward new methods of rapid and facile ee analysis.[10]

Understanding how CSAs differentiate enantiomers by NMR is essential both to their optimal use and to the rational design of improved variants. Because the association/dissociation kinetics of many binding processes are fast on NMR time scales, experiments employing CSAs typically yield NMR spectra of weighted averages of free and bound species.[8a,b,11] Consequently, enantiodiscrimination may arise from energetic and/or spectral (magnetic) differences between diastereomeric substrate:CSA complexes. If one substrate enantiomer is bound more strongly by the CSA (energetic discrimination), that enantiomer will be complexed to a greater degree in a competitive regime in which the substrate is present in excess over the CSA. In such cases, discrimination may be observed even if the limiting bound chemical shifts of the diastereomeric complexes are very similar. On the other hand, if the inherent NMR spectra of the diastereomeric complexes differ significantly (spectral discrimination), discrimination will result even when both are present in similar amounts, for example, once the substrate has been saturated with the CSA. An ideal CSA would provide useful levels of differentiation over wide stoichiometric and concentrations ranges, thus allowing for substoichiometric use but not requiring the achievement of any specific molar ratios.

Herein, we report the synthesis of a series of chiral aza-crown macrocycles, of which each member contains a di(*N*-benzylated) *trans*-1,2-diaminocyclohexane (DACH) subunit. X-ray crystal structures of several macrocycles are presented, along with evidence of enantiomeric discrimination of mandelic acid (MA) derivatives by ^{1}H NMR spectroscopy in chloroform. Binding studies indicate that the macrocycles generally form simultaneous 1:1 and 2:1 complexes with the enantiomers of MA, which are driven by interactions between the amine and carboxylic acid groups of the macrocycles and substrates, respectively. In most cases, the 2:1 MA:macrocycle complexes are found to be responsible for the observed enantioselectivity. Several of the macrocycles are shown to function as effective CSAs for MA derivatives, allowing for the accurate determination of ee by ^{1}H NMR spectroscopy.

■ DESIGN CRITERIA

As a byproduct of industrial nylon production, DACH is an inexpensive and ubiquitous chiral subunit[12] that has been widely incorporated into schemes for enantioselective molecular recognition,[2d,5e,11a,c,13] synthesis,[14] sensing,[4i,15,16] and separation.[17] Structurally, DACH is preorganized by a preferred diequatorial conformation, which persists in water regardless of protonation state,[18] and presumably enhances its efficacy as a chelating Lewis base (ca. 3-fold higher affinity than ethylenediamine for Zn(II), Cu(II), and Ni(II)[19]). The elaboration of the N atoms is a general strategy for the creation of chiral molecular clefts centered on the vicinal diamine group. In particular, di(*N*-benzylated) DACH derivatives and related compounds have been highly successful as ligands for asymmetric catalysts[14a,14c] and as enantioselective receptors.[2d,4i,11b,16a] Our interest in the effects of constraining the *N*-benzylated DACH subunit within macrocyclic systems led us to prepare the compounds shown in Figure 1. Although numerous highly symmetrical chiral macrocycles comprised of multiple *N*-benzylated DACH subunits[2d,8f,16,20] have been reported, macrocycles containing a single DACH unit,[21,22] which may be more amenable to investigations of binding phenomena, have been less well studied.

Figure 1 shows the structures of the receptors described in this study. With the exception of (*R*,*R*)-**8**, which serves as a nonmacrocyclic control compound, each receptor contains a DACH moiety that is joined through *N*-benzylic linkages to a flexible oligoethylene glycol bridge. The DACH subunits

dx.doi.org/10.1021/jo2018203 | J. Org. Chem. 2011, 76, 10020–10030

Scheme 1. (A) Representative Synthesis of (*R*,*R*)-5;[a] (B) Intermediate Compounds Used in the Syntheses of the Macrocycles Shown in Figure 1

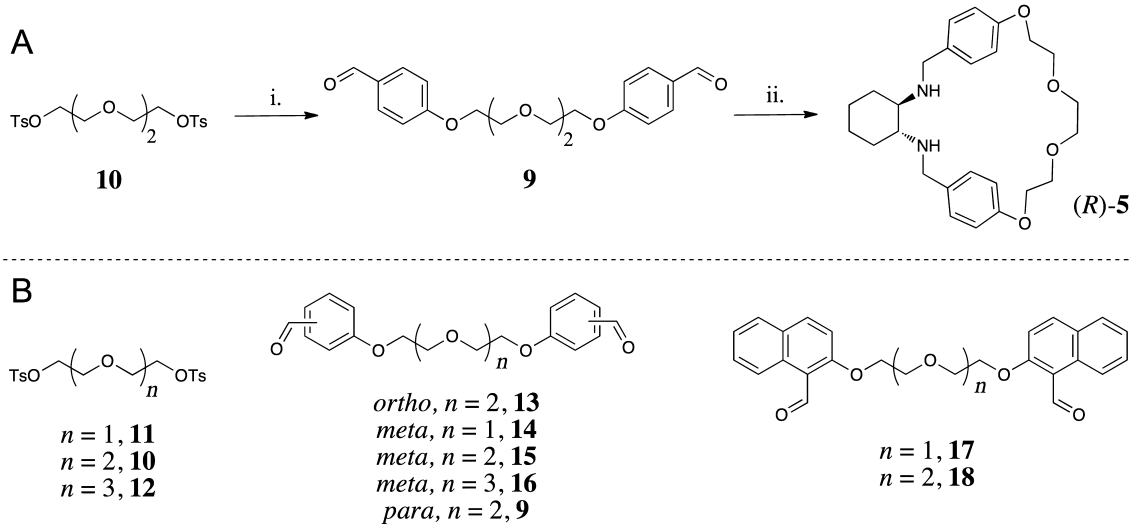

[a]Reagents: (i) *p*-hydroxybenzaldehyde, K_2CO_3, NaI, MeCN; (ii) (a) (*R*,*R*)-1,2-diaminocyclohexane, MeOH, (b) $NaBH_4$.

impart chirality and C_2 symmetry onto the structures, while directing the vicinal amino groups toward the interior of relatively rigid clefts enforced by the arene spacers. With the exception of compounds (*R*,*R*)-**1**[21] and the non-macrocyclic control compound (*R*,*R*)-**8**,[15] the receptors described here are, to the best of our knowledge, previously unreported. The *ortho*-linked naphthyl groups of (*R*,*R*)-**6** and (*R*,*R*)-**7** are derived from readily available 2-hydroxy-1-naphthaldehyde and are expected to increase the steric bulk about the DACH center relative to the *ortho*-phenylene group of (*R*,*R*)-**1**, while potentially enabling fluorescence monitoring of binding events in future work. The arene linkage geometry and length of the oligoethylene glycol bridge will influence the overall shape and flexibility of the macrocycles and, in turn, their binding properties. However, Smithrud et al. have shown that for a related series of di(*N*-benzylated) DACH-containing cyclophanes the arene linkage geometry significantly affects the basicity of the amino groups by allowing for differing degrees of solvation and cation−π stabilization of the conjugate acid ammonium ions,[22a] which implies that both steric and electronic factors may contribute to changes in binding properties that accompany structural variations among the macrocycles.

RESULTS AND DISCUSSION

Synthesis. Each of the macrocycles was prepared as a single enantiomer according to routes analogous to that shown for (*R*,*R*)-**5** in Scheme 1A. The dialdehyde **9** was prepared from the corresponding ditosylate **10** and cyclized with optically pure (*R*,*R*)-DACH through a reductive amination protocol. Under suitably dilute conditions, this approach reliably yielded the desired [1 + 1] macrocycles as the major product, although [2 + 2] products were occasionally detected in crude reaction mixtures by thin layer chromatography and mass spectrometry. In all cases, the NMR spectra demonstrate the expected C_2 symmetry, and no surprising correlations were observed in the NOESY spectra. The structures of intermediate compounds used in the preparation of the remaining macrocycles are shown in Scheme 1B.

Structural Analysis. The structures of four of the macrocycles shown in Figure 1 were determined by X-ray crystallography using a Cu-based X-ray source that allows for independent confirmation of absolute configuration. Figure 2 shows ORTEP diagrams for the series of *meta*-linked macrocycles (*R*,*R*)-**2**, (*R*,*R*)-**3**, and (*R*,*R*)-**4**. All of the structures display intramolecular hydrogen bonding between the vicinal amino groups and *gauche* relationships between both benzylic C atoms and the nearest cyclohexyl methine H atoms. The smallest macrocycle (*R*,*R*)-**2** (Figure 2A) adopts a conformation in which both phenylene rings reside *anti* to the respective adjoining cyclohexyl ring C atoms (dihedral angles: C6−N2−C24−C22 = 179°; C1−N1−C7−C8 = 173°), giving the molecule a relatively planar overall shape, whereas the larger macrocycles (*R*,*R*)-**3** and (*R*,*R*)-**4** (Figure 2B,C) exhibit near-perpendicular arrangements of the two phenylene rings (73° and 80° angles for (*R*,*R*)-**3** and (*R*,*R*)-**4**, respectively), which in both cases is caused by *gauche* relationships between one of the phenylene rings and the nearest cyclohexane C atom attached to the intramolecular hydrogen bond donor N−H group (dihedral angle for (*R*,*R*)-**3**: C21−N21−C27−C28 = 58°; for (*R*,*R*)-**4**: C1−N1−C7−C8 = 57°). In addition to the intramolecular hydrogen bonding seen in all of the structures, (*R*,*R*)-**2** features intermolecular N−H···N hydrogen bonding that runs in two different directions within the crystal, thus producing "methylene-like" disorder of the N−H bonds (omitted from Figure 2A). These interactions are presumably facilitated by the approximate planarity of (*R*,*R*)-**2**, as intermolecular hydrogen bonding is absent in the structures of (*R*,*R*)-**3** and (*R*,*R*)-**4**.

The crystal structures shown in Figure 2 are thought to reflect the increasing flexibility of the *meta*-linked macrocycles with ring size. Molecular modeling[23] suggests that (*R*,*R*)-**2** is relatively rigid and that *anti* conformations are required about both benzylic C−N bonds (*anti-anti* conformation) to avoid excessive strain within the macrocycle. As a consequence, the two chemically equivalent aryl H atoms that reside *ortho* to both ring substituents (referred to as *diortho*) are firmly directed toward the interior of the macrocyclic cavity of (*R*,*R*)-**2** and constrained within the anisotropic deshielding region of the

dx.doi.org/10.1021/jo2018203 | J. Org. Chem. 2011, 76, 10020−10030

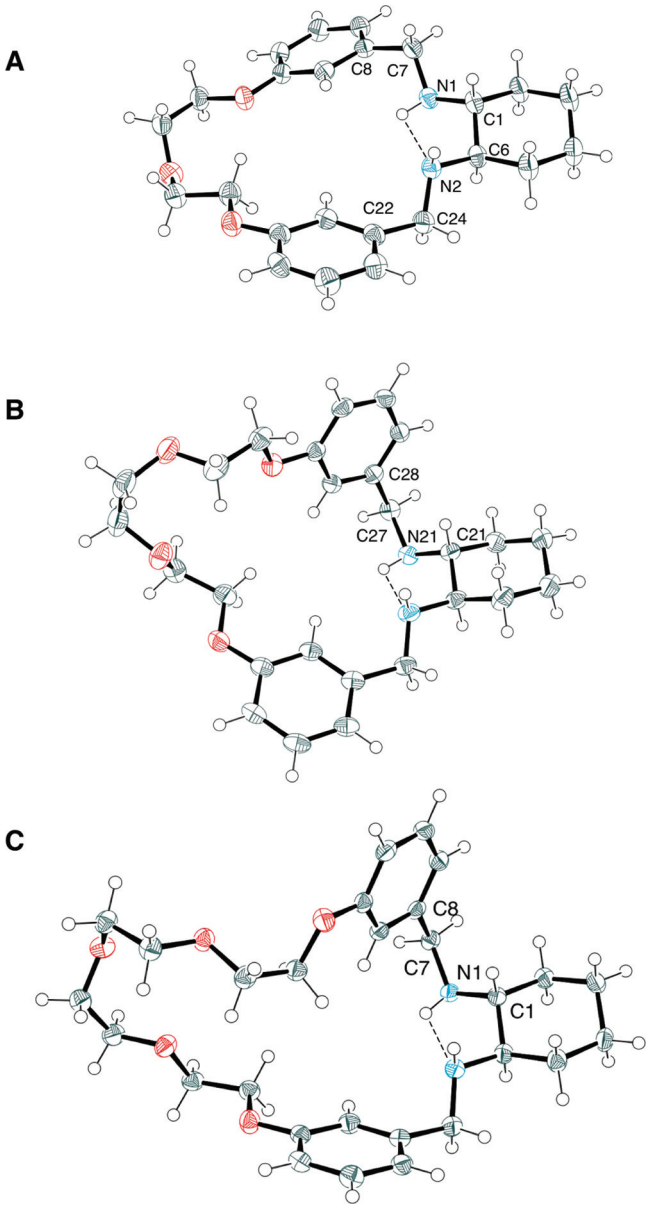

Figure 2. Views of the ORTEP diagrams of (A) (*R*,*R*)-**2**, because of disorder caused by intramolecular H-bonding, four N−H bonds were observed, of which two are omitted, (B) (*R*,*R*)-**3** and (C) (*R*,*R*)-**4**; thermal ellipsoids are scaled to 50% probability.

transannular arene ring. However, the more flexible macrocycles (*R*,*R*)-**3** and (*R*,*R*)-**4** are capable of accessing conformations in which one of the benzylic C−N bonds is *gauche* (*anti-gauche*, as observed in the X-ray structures and predicted by molecular modeling), which allows the two phenylene rings to move apart, thus diminishing transannular deshielding anticipated in the *anti-anti* conformation. As expected on this basis, the ^{1}H NMR chemical shifts of the *diortho* H resonances vary considerably among the series, with a significant upfield shift observed with increasing ring size (see Figure S-15). This is taken as evidence that within the *meta*-linked series, the *anti-gauche* conformation becomes more accessible as the length of the flexible oligoethylene glycol linker increases and that conformational flexibility about the DACH-centered cleft increases appreciably in the order (*R*,*R*)-**2** < (*R*,*R*)-**3** < (*R*,*R*)-**4**.

Figure 3 shows the ORTEP diagram of (*R*,*R*)-**7**, determined from crystals grown from a concentrated $CDCl_3$ solution. A single solvent of crystallization is present in the structure and has been omitted for clarity. The two naphthyl rings of (*R*,*R*)-**7** are nearly parallel (16.7° angle) and are oriented away from the cyclohexyl group (dihedral angles: C1−N2−C34−C29 = 166°; C6−N1−C7−C8 = 179°), defining a cleft in which the vicinal diamines reside. This cleft is further arranged in a pseudosymmetrical fashion by the *gauche* relationship between both N-benzyl bonds and their respective cyclohexyl methine H atoms, as observed in all structures in Figure 2. The vicinal amino groups participate in an internal hydrogen bond (N1−N2 distance = 2.792 Å), which is bifurcated through an interaction with one of the aryl ether oxygen atoms (N1−O1 distance 2.952 Å, Figure 3B). The *ortho*-linkage geometry causes the triethylene glycol chain to span the naphthyl rings on one side of the average plane of the cyclohexyl moiety, imparting a pronounced kink onto the 20-membered ring.

Chirality Recognition. The receptors shown in Figure 1 were evaluated as CSAs for MA, which has been widely used as a model substrate for enantioselective recognition studies.[4d,e,h,5d,n,7b,8d−g,j,16b,20c,24] The addition of a receptor to a solution of racemic MA in $CDCl_3$ caused the benzylic C−*H* resonance in the ^{1}H NMR spectrum of MA to shift upfield and, in most cases, to split into two equal-intensity singlets that drift downfield slightly and reconverge as [receptor]/[MA] approaches unity. Representative spectra for the most effective compound (*R*,*R*)-**4** are presented in Figure 4A. The two singlets are assigned to the MA enantiomers, which become desymmetrized through their interaction with the macrocycle.

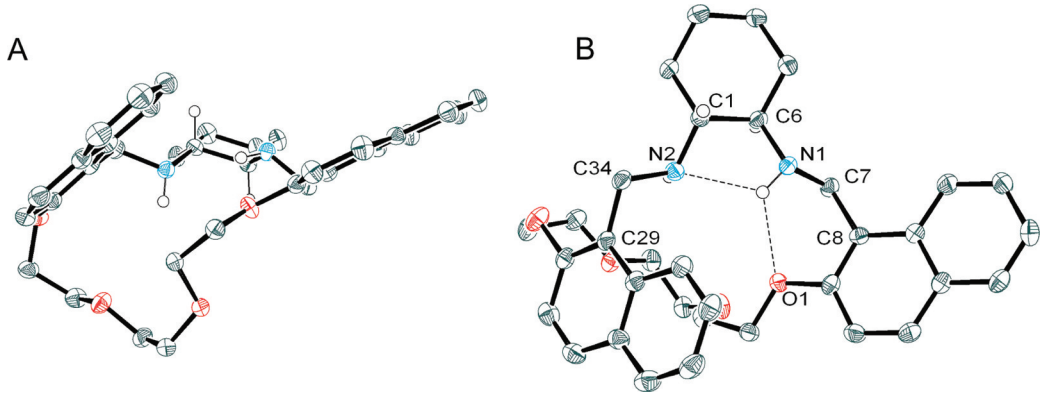

Figure 3. Side (A) and top (B) views of the ORTEP diagram of (*R*,*R*)-**7**. Thermal ellipsoids are scaled to 50% probability. Most of the hydrogen atoms and a $CDCl_3$ molecule of crystallization have been omitted for clarity.

dx.doi.org/10.1021/jo2018203 | *J. Org. Chem.* 2011, 76, 10020−10030

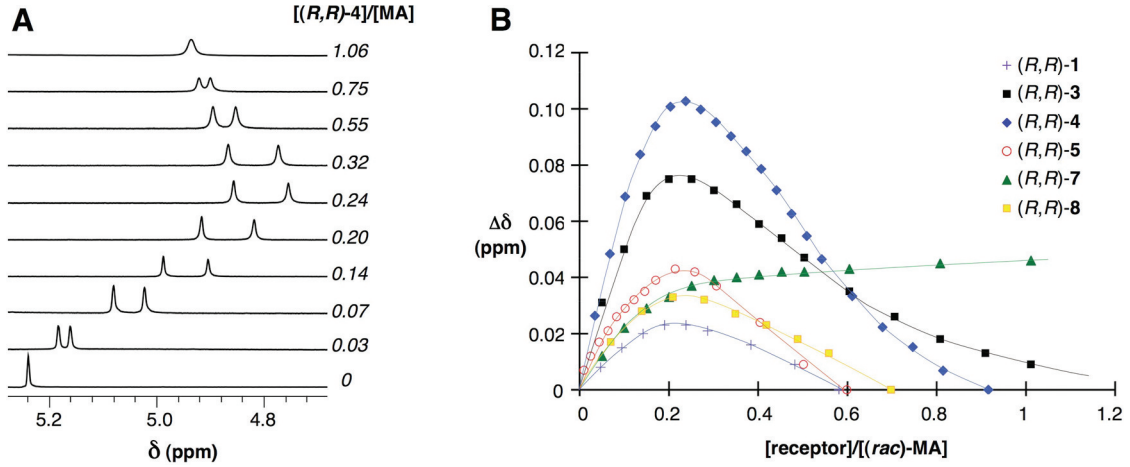

Figure 4. (A) Variations in part of the 300 MHz ^{1}H NMR spectrum corresponding to the benzylic C−*H* resonance of (*rac*)-mandelic acid (MA, 10.0 mM in $CDCl_3$) upon increasing [(*R*,*R*)-**4**]; additional studies of optically pure MA samples reveal that (*R*)-MA undergoes the greater upfield shift. (B) Chemical shift nonequivalencies ($\Delta\delta$) of the enantiomeric α-H signals of (*rac*)-MA (10.0 mM in $CDCl_3$) as a function of molar ratio for the effective receptors; curves intended only to guide the eye; spectra collected at 23 °C.

Scheme 2. A Proposed Simultaneous 1:1 and 2:1 Binding Model for the Interaction of Mandelic Acid and (*R*,*R*)-3[a]

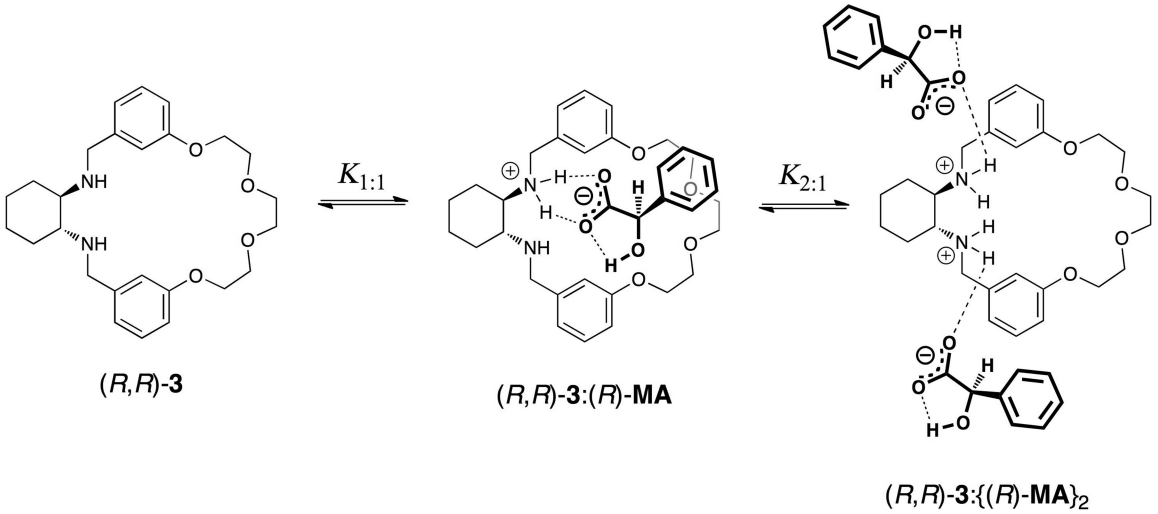

[a]Binding geometries and protonation states are speculative.

As expected, analogous experiments performed with enantiomerically pure MA samples yielded similar chemical shift variations, but no splitting of the signals, and indicated that (*R*)-MA undergoes the larger upfield shift. The overall upfield shift of the benzylic C−*H* resonance, and the fact that the most significant corresponding changes in the ^{1}H NMR spectrum of (*R*,*R*)-**4** are downfield shifts of N−C−*H* signals (see Figure S-17), suggest that the effect is driven primarily by Brønsted−Lowery acid/base interactions between the carboxylic acid and amine groups of the substrate and receptor, respectively. The observed chemical shift dependence of the benzylic C−*H* resonance on molar ratio (first upfield and then slightly downfield) is uncommon among CSAs[8b] and likely signifies a binding stoichiometry beyond a simple 1:1 complexation. The maximal chemical shift difference between the signals ($\Delta\delta$) achieved in Figure 4A is roughly 0.1 ppm, and baseline resolution is sustained over a fairly wide [(*R*,*R*)-**4**] range (ca. 0.5−6.5 mM), thus demonstrating the potential of this macrocycle as a CSA for MA.

Figure 4B plots the chemical shift nonequivalencies ($\Delta\delta$) of MA enantiomers observed for each receptor as a function of molar ratio. In most cases, the enantiomeric separation increases sharply as the molar ratio rises from 0 to about 0.25 and then steadily declines to zero as [receptor]/[(*rac*)-MA] is increased further. The naphthyl-containing macrocycle (*R*,*R*)-**7** represents an exception to this trend, as saturation of $\Delta\delta$ is observed near [(*R*,*R*)-**7**]/[(*rac*)-MA] = 0.25. No observable enantiodiscrimination was provided by the smaller diethylene glycol-linked macrocycles (*R*,*R*)-**2** and (*R*,*R*)-**6** under the conditions studied. Apparently, the smaller cavities of these receptors do not allow for inclusion of MA to the extent that molecular shape can be efficiently discriminated. It is evident from Figure 4B that, among the series of isomeric triethylene glycol-linked macrocycles, the *meta*-linkage of (*R*,*R*)-**3** provides the greatest enantiodiscrimination, whereas the *ortho*- and *para*-linked compounds (*R*,*R*)-**1** and (*R*,*R*)-**5** are not significantly more effective than the non-macrocyclic receptor (*R*,*R*)-**8**. Within the series of *meta*-linked ((*R*,*R*)-**2**, (*R*,*R*)-**3**, and (*R*,*R*)-**4**) and naphthyl-linked ((*R*,*R*)-**6** and (*R*,*R*)-

dx.doi.org/10.1021/jo2018203 | J. Org. Chem. 2011, 76, 10020−10030

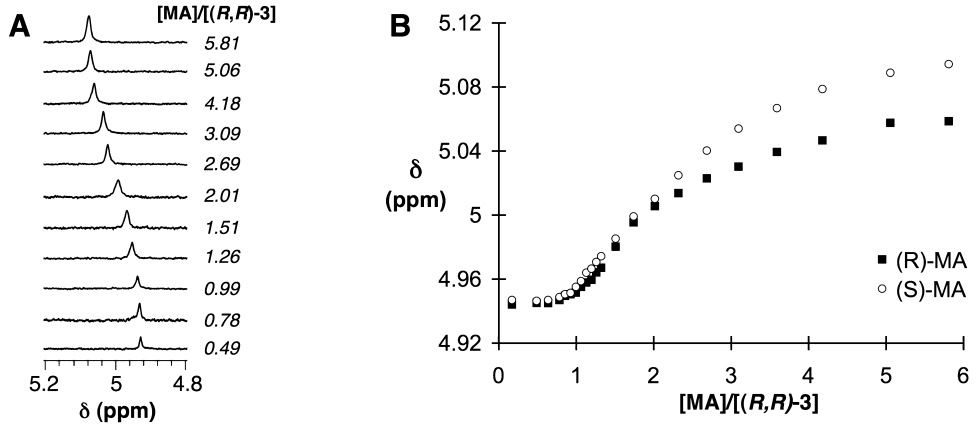

Figure 5. (A) Variations in the region of the 300 MHz ^{1}H NMR spectrum corresponding to the benzylic C–*H* of (*S*)-mandelic acid ((*S*)-MA, varying concentration), in the presence of (*R*,*R*)-**3** (440 μM). (B) Binding isotherms for (*S*)-MA and (*R*)-MA under conditions from (A); spectra collected in $CDCl_3$ at 23 °C.

Table 1. Limiting Bound Chemical Shifts and Macroscopic 2:1 Binding Constants[a]

	limiting bound chemical shifts (ppm)				2:1 binding constants (M^{-1})	
receptor	$\delta_{1:1}(R)$	$\delta_{1:1}(S)$	$\delta_{2:1}(R)$	$\delta_{2:1}(S)$	$K_{2:1}(R)$	$K_{2:1}(S)$
(*R*,*R*)-**1**	4.92	4.90	3.84	3.68	$(3.3 \pm 0.5) \times 10^2$	$(1.9 \pm 0.3) \times 10^2$
(*R*,*R*)-**2**	4.93	4.93	4.96	4.96	$(4.8 \pm 0.7) \times 10^3$	$(5.6 \pm 0.8) \times 10^3$
(*R*,*R*)-**3**	4.94	4.94	2.99	4.42	$(2.2 \pm 0.5) \times 10^2$	$(7.4 \pm 1.1) \times 10^2$
(*R*,*R*)-**6**	4.97	4.96	4.52	4.64	$(7.5 \pm 1.2) \times 10^2$	$(9.3 \pm 1.4) \times 10^2$
(*R*,*R*)-**7**	4.84	4.89	4.51	4.11	$(9.6 \pm 1.5) \times 10^2$	$(1.8 \pm 0.3) \times 10^2$

[a]Determinations carried out in $CDCl_3$ at 23 °C by fitting binding isotherms such as those shown in Figure 5B with the computer program NMRTit HGG; the determined $K_{1:1}$ values are too large for accurate analysis by ^{1}H NMR.[27]

7) macrocycles, enantiodiscrimination is shown to increase with ring size, and additionally, the greater effectiveness of (*R*,*R*)-**7** relative to (*R*,*R*)-**1** demonstrates the beneficial affect of the naphthyl groups in the *ortho*-linked system.

The variations in $\Delta\delta$ with molar ratio shown in Figure 4B can be tentatively explained in terms of a binding model in which (*rac*)-MA simultaneously forms complexes with the receptors of both 2:1 and 1:1 stoichiometries, and with the exception of (*R*,*R*)-**7**, only the ternary complexes exhibit significant enantioselectivity. The occurrence of both 2:1 and 1:1 complexes, as depicted in Scheme 2 for (*R*,*R*)-**3**, is consistent with the assumption that proton transfer and/or hydrogen bonding drive the association and has been previously reported for the enantioselective recognition of MA by a calix[4]arene bearing two chiral amine subunits.[24f] In that study also, the 2:1 MA:receptor complexes were determined to be the major source of enantioselectivity. In addition, (*R*,*R*)-1,2-diphenylethane-1,2-diamine is known to be most effective as a CSA for chiral carboxylic acids at a carboxylic acid:diamine ratio of 2:1.[8j] Early in the titrations represented in Figure 4B, as the molar ratio proceeds from 0 to 0.25, 2:1 complexes are statistically favored by stoichiometry imbalance. Throughout this range, there is sufficient MA to allow the receptor to selectively bind the enantiomer that forms the more stable 2:1 complex, while preferentially leaving its antipode free in solution. As the molar ratio further increases from 0.25 to 0.5, 2:1 complexes remain statistically favored, and so the majority of receptor added over this regime may interact with the leftover, weaker-binding MA enantiomer in a 2:1 fashion, causing a convergence of the chemical shifts. As the molar ratio proceeds from 0.5 through unity, 1:1 complexes become increasingly significant, and assuming these to be spectroscopically similar, the enantiodiscrimination would diminish. The persistence of nonequivalence over this range for the macrocycle (*R*,*R*)-**7** implies that for this macrocycle the diastereomeric 1:1 complexes are thermodynamically and/or magnetically dissimilar, which is likely the result of increased steric demand and/or magnetic anisotropy about the binding site provided by the naphthyl rings. While the overall analysis presented above neglects the involvement of heterochiral ternary complexes (e.g., (*R*)-MA:(*R*,*R*)-**3**:(*S*)-MA), the observed $\Delta\delta$ maxima near [receptor]/[(*rac*)-MA] = 0.25 nevertheless qualitatively support 2:1 MA:macrocycle complexes as the major source of chirality discrimination.

Additional ^{1}H NMR experiments were performed in which the concentrations of single enantiomers of MA were gradually increased in the presence of constant concentrations of the macrocycles. As before, the chemical shift of the benzylic C-*H* resonance of MA was monitored as a function of molar ratio, defined here as the inverse of that from Figure 4. Figure 5 shows typical results, in the case where [MA]/[(*R*,*R*)-**3**] is raised incrementally from ~0.2 to ~6.0. The chemical shift variations shown in Figure 5B exhibit changes in slope near [MA]/[(*R*,*R*)-**3**] = 1 and [MA]/[(*R*,*R*)-**3**] = 2, which provides evidence for the formation of both 1:1 and 2:1 complexes.[25] It is generally observed that when the substrate:macrocycle ratio is <1, δ is quite insensitive to the molar ratio, as virtually all of the MA present under these conditions is expected to bind the macrocycle in a 1:1 fashion (provided $1/K_{1:1} < [(R,R)\text{-}3]_t$ = 440 μM). The δ value observed when the receptor is in great excess over MA is therefore considered to be close to the limiting bound chemical shift of the 1:1 complex (*R*,*R*)-**3**:MA. The coincidence of chemical shifts for MA enantiomers over this range confirms the nonselectivity of 1:1 complexes, and as

dx.doi.org/10.1021/jo2018203 | J. Org. Chem. 2011, 76, 10020–10030

expected, is observed for all of the macrocycles except (*R*,*R*)-**7** (see Figure S-24). As [MA]/[(*R*,*R*)-**3**] increases beyond unity, the signals initially shift downfield sharply and diverge, while gradually approaching saturation at higher molar ratios. This behavior is interpreted in terms of the accumulation of unbound MA along with the gradual onset of spectroscopically and/or energetically distinct 2:1 complexes when MA is present in significant excess.

The chemical shift variations shown in Figure 5B were fitted to the model depicted in Scheme 2 using the computer program NMRTit HGG,[26] which provides estimates of $K_{1:1}$, $K_{2:1}$, and the associated limiting bound chemical shifts $\delta_{1:1}$ and $\delta_{2:1}$. The excellent fits obtained for most macrocycles (see Supporting Information) confirm the proposed binding model in those cases, but the determined $K_{1:1}$ values are on the order of 10^5–10^6 M^{-1}, which are too large to be directly quantified by NMR.[27] However, the $K_{2:1}$ values were reproducibly determined and are presented along with the corresponding limiting bound chemical shifts in Table 1. Of the receptors for which binding constants were measured, (*R*,*R*)-**7** show the greatest binding enantioselectivity, with differences in 2:1 binding free energies of ∼1 kcal mol^{-1} between MA enantiomers. Binding parameters were not obtained for receptors (*R*,*R*)-**4** and (*R*,*R*)-**5**, as the latter showed significant variations in δ with molar ratio for both MA enantiomers when [MA]/[(*R*,*R*)-**5**] < 1 (Figure S-22) and the former displayed an anomalous discontinuity in the binding isotherm of (*R*)-MA at [MA]/[(*R*,*R*)-**4**] = 1.5 (Figure S-21), suggesting that the binding equilibria operative in these systems may be more complicated than that depicted in Scheme 2. Despite the unavailability $K_{1:1}$ values, in most cases the strong correlations between experimental and theoretical binding isotherms, and the similarity of $\delta_{1:1}$ values between enantiomers further implicates the 2:1 complexes as the major source of chirality discrimination.

Although the involvement of ternary complexes obscures a structural analysis of binding enantioselectivity in these systems, rudimentary structural information was obtained through nuclear Overhauser effect spectroscopy (NOESY). 2D NOESY spectra of the complexes of (*rac*)-MA with (*R*,*R*)-**2**, (*R*,*R*)-**3**, (*R*,*R*)-**4**, and (*R*,*R*)-**7** were collected under conditions of maximal chemical shift nonequivalence. The presence of the *meta*-linked macrocycles ((*R*,*R*)-**2**, (*R*,*R*)-**3**, and (*R*,*R*)-**4**) was found to increase the solubility of MA in $CDCl_3$ by about an order of magnitude, whereas (*R*,*R*)-**7** did not influence MA solubility appreciably. Under conditions of increased concentrations, much stronger intermolecular NOEs were observed, and for (*R*,*R*)-**3** and (*R*,*R*)-**4**, substantially larger benzylic C–*H* resonance nonequivalencies were achieved ($\Delta\delta$ = 0.098 and 0.125 ppm for (*R*,*R*)-**3** and (*R*,*R*)-**4**, respectively, at [MA] = ca. 100 mM). The complexes of all four macrocycles showed intermolecular NOEs between the enantiomeric benzylic C–*H* resonances of MA and the diastereomeric benzylic C–*H* resonances of the macrocycles, with more intense correlations to the pro-*S* H atoms of the macrocycles (H_a in Figure 6). A portion of the NOESY spectrum of the (*rac*)-MA:(*R*,*R*)-**7** complexes at a near 1:1 molar ratio is shown in Figure 6. The benzylic C–*H* resonances of both MA enantiomers are correlated with the H_a signal (circled in blue), but only that of the stronger-binding (*R*)-MA correlates to H_b (green). This result confirms that the MA enantiomers are bound by (*R*,*R*)-**7** in structurally distinct environments and suggests that (*R*)-MA forms the tighter 1:1 complex. Similar analyses of MA

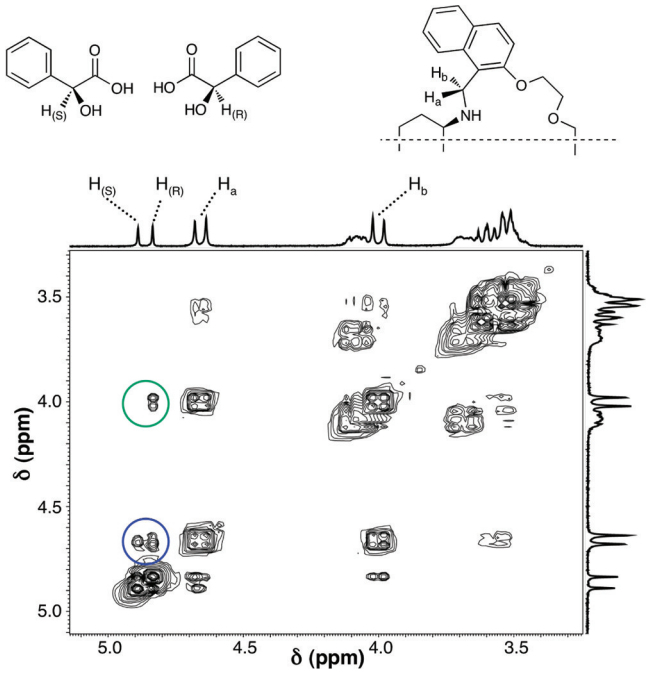

Figure 6. A portion of the 300 MHz NOESY spectrum of a solution of (*rac*)-mandelic acid (8.70 mM) and (*R*,*R*)-**7** (9.04 mM) in $CDCl_3$ at 23 °C; intermolecular correlations to H_a and H_b are circled in blue and green, respectively; assignments of H_a and H_b made on the basis of an intramolecular NOE correlation of H_b with the cyclohexyl methine proton.

complexes with (*R*,*R*)-**3** and (*R*,*R*)-**4** also reveal nonequivalent intermolecular NOEs between MA enantiomers; however, the differences between MA enantiomers are less prominent (see Figures S-26 and S-27).

Several of the macrocycles were tested as CSAs for a range of MA derivatives, for which maximal $\Delta\delta$ values are presented in Table 2. For each macrocycle, the variations in $\Delta\delta$ with molar ratio were qualitatively similar to those presented for MA in Figure 4B, with maximal $\Delta\delta$ near [receptor]/[MA] = 0.25 for (*R*,*R*)-**3**, (*R*,*R*)-**4**, and (*R*,*R*)-**5** and near saturation of $\Delta\delta$ occurring at [(*R*,*R*)-**7**]/[MA] > 0.25 (see also Figure S-28).

Table 2. Maximal Chemical Shift Nonequivalencies for Mandelic Acid Derivatives[a]

	receptor			
guest	(*R*,*R*)-**3**	(*R*,*R*)-**4**	(*R*,*R*)-**5**	(*R*,*R*)-**7**
MA	0.077	0.102	0.043	0.054
ortho-Cl-MA	0.077	0.079	0.047	0.033
meta-Cl-MA	0.060	0.074	0.046	0.052
para-Cl-MA	0.114	0.130	0.034	0.048
para-Br-MA	0.078	0.128	0.042	0.038
para-OMe-MA	0.090	0.105	0.022	0.032
α-MPA	0	0.025	0.030	0.031

[a] ^{1}H NMR chemical shift differences ($\Delta\delta$, ppm) between the benzylic C–*H* resonances of enantiomers of (*rac*)-mandelic acid (MA) derivatives (ca. 10 mM) observed upon titration of macrocycles in $CDCl_3$ at 23 °C. Entries in bold denote the achievement of clear baseline resolution of signals on a 300 MHz instrument. For each macrocycle and MA derivative, variations in $\Delta\delta$ with molar ratio were qualitatively similar to those shown for MA in Figure 4B. α-MPA = α-methoxyphenylacetic acid.

dx.doi.org/10.1021/jo2018203 | *J. Org. Chem.* 2011, 76, 10020–10030

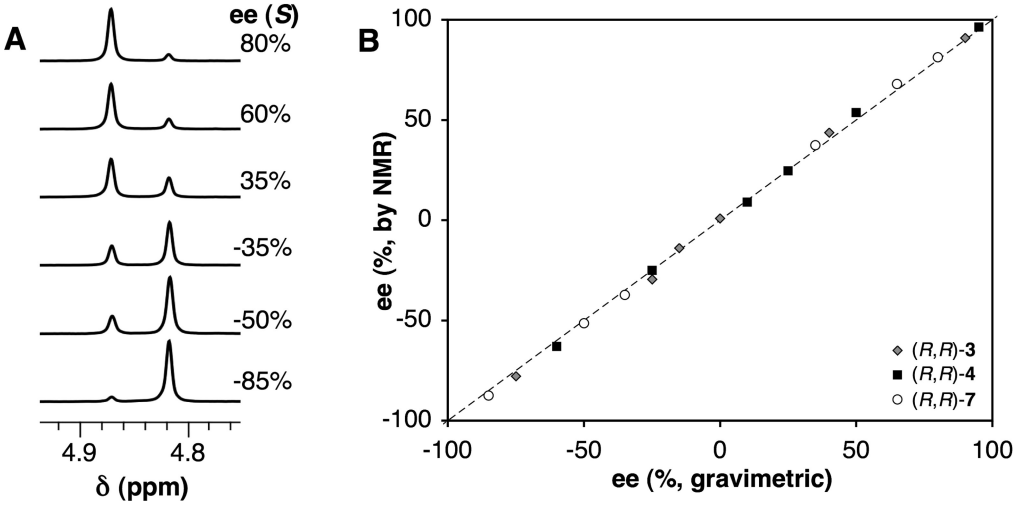

Figure 7. (A) Portion of the 300 MHz ^{1}H NMR spectra of nonracemic mandelic acid samples (8.7 mM, various ee values) and (*R*,*R*)-7 (8.5 mM) in $CDCl_3$. (B) Correlation between ee values determined gravimetrically and by integration of the signals such as those shown in (A); ee defined in terms of (*S*)-MA.

The larger *meta*-linked macrocycles (*R*,*R*)-**3** and (*R*,*R*)-**4** are the most widely successful of those studied and are capable of resolving enantiomeric signals for a variety of arene-substituted MA derivatives, with especially large nonequivalencies observed for *para*-substituted compounds. The poor differentiation generally observed toward the enantiomers of α-methoxyphenylacetic acid (α-MPA) implies that hydrogen bond donation by the α-hydroxyl group of MA is crucial for enantiodiscrimination. None of the macrocycles tested elicited changes in the ^{1}H NMR spectrum of (*rac*)-methyl mandelate, thus providing further support for a binding model involving proton transfer or hydrogen bonding.

In order to demonstrate the practical utility of the macrocycles as CSAs, ee values of multiple nonracemic MA samples were determined by integration of the enantiomeric benzylic C−*H* resonances in the presence of near-optimal quantities of receptors (*R*,*R*)-**3**, (*R*,*R*)-**4**, and (*R*,*R*)-**7**. Figure 7 shows that (*R*,*R*)-**7**, which provides the smallest enantiodiscrimination of the three macrocycles employed, maintains analytical resolution over a wide ee range and that each of the three macrocycles yields an excellent correlation between the ee values determined by NMR and those determined gravimetrically. The average absolute error in the 18 ee measurements plotted in Figure 7B is ∼1%. Further, a consistent relationship between the chemical shifts and the configuration of MA was observed among the three macrocycles tested, with (*R*)-MA undergoing the greater upfield shift in each case.

SUMMARY

A series of new, enantiomerically pure DACH-based macrocycles containing arene and oligo(ethylene glycol) spacers have been prepared, and four members have been characterized by X-ray crystallography. Most of the macrocycles were found to enantioselectively associate with MA by ^{1}H NMR on the basis of interactions between the carboxylic acid and amine groups of the substrates and macrocycles, respectively. The abilities of the macrocycles to differentiate the ^{1}H NMR spectra of the enantiomers of MA by binding in $CDCl_3$ was found to be markedly dependent on (1) the nature of the arene group, (2) the arene linkage geometry, and (3) the length of the oligo(ethylene glycol) bridge. ^{1}H NMR studies demonstrate that in most cases MA binds to the macrocycles to form complexes of both 1:1 and 2:1 stoichiometry and that the 2:1 complexes generally provide the source of enantiodiscrimination. ^{1}H NMR titration data yielded estimates of 2:1 binding constants to several of the macrocycles; however, the 1:1 binding constants are too large to be quantified by this method. Differential intramolecular NOEs were observed between the enantiomers of MA and the most effective macrocycles. The *meta*-linked macrocycles (*R*,*R*)-**3** and (*R*,*R*)-**4** as well as the naphthyl-containing *ortho*-linked macrocycle (*R*,*R*)-**7** are shown to be effective CSAs for MA derivatives and derivatives and were used to accurately determine the ee of a number of MA samples.

EXPERIMENTAL SECTION

General. ^{1}H NMR spectra were recorded at 300 MHz and are referenced to the solvent. Analytical thin layer chromatography was performed using 0.2 mm silica gel plates. Column chromatography was performed with silica gel 60 (230−400 mesh). Reagents were used as received from commercial suppliers. All reactions were carried out under an atmosphere of dry N_2. Anhydrous CH_2Cl_2 was obtained by passage through columns of activated molecular sieves. Acetonitrile was distilled over P_2O_5. Anhydrous methanol was prepared by stirring for 12 h over 3 Å molecular sieves. Ammonia-saturated methanol was obtained by bubbling $NH_{3(g)}$ through anhydrous methanol (500 mL) for 45 min at 0 °C. Anhydrous K_2CO_3 was stored at 110 °C for at least 72 h prior to use and allowed to cool in a desiccator. (*R*,*R*)-DACH was resolved according to literature precedent,[28] free-based from the L-tartrate salt, and used immediately. Compounds (*R*,*R*)-**8**[15] and **10**−**12**[29] were prepared according to literature precedent. Yields refer to homogeneous, analytically pure (^{1}H NMR) material and have not been optimized.

^{1}H NMR Analyses. $CDCl_3$ was passed through a column of activated alumina prior to use, although virtually identical chemical shift nonequivalencies were achieved when untreated $CDCl_3$ was used. Enantiodiscrimination studies of *rac*-MA derivatives (Figure 4 and Table 2) were carried out by adding small aliquots of the macrocycle stock solution (typically near 200 mM in $CDCl_3$) to an NMR tube containing of the MA derivative (550 μL and typically near 10 mM), so that changes in the analyte solution volume were small (<5%). Binding titrations (Figure 5 and Table 1) were performed by mixing stock solutions of enantiomerically pure MA (typically near 8 mM in $CDCl_3$) and a given macrocycle (typically near 200 mM in $CDCl_3$) to

dx.doi.org/10.1021/jo2018203 | J. Org. Chem. 2011, 76, 10020−10030

obtain an analyte solution (typically 1 mL and near 500 μM macrocycle in $CDCl_3$) and a titrant solution (typically 5 mM in MA and always of identical macrocycle concentration as present in the analyte solution; also in $CDCl_3$), thus ensuring that the macrocycle concentration remained constant over the course of the experiment. Titrations of a given macrocycle with enantiomeric MA samples were performed in parallel. The observed chemical shift changes were fitted with the computer program NMRTit HGG.[26] The macroscopic 2:1 binding constants reported in Table 1 have been statistically corrected[30] from those reported by NMRTit HGG to account for the fact that the program returns microscopic binding constants.

Crystallographic Data Collection and Refinement. Crystals of (*R*,*R*)-**2** and (*R*,*R*)-**3** were grown by evaporation from concentrated Et_2O solutions, whereas crystals of (*R*,*R*)-**4** and (*R*,*R*)-**7** were obtained by slow evaporation from solutions in $CDCl_3$. X-ray diffraction data were collected on a CCD platform diffractometer (Cu Kα (λ = 1.541 78 Å)) at 125 K. Crystals were mounted in a nylon loop with cryoprotectant oil. The structures were solved using direct methods and standard difference map techniques and were refined by full-matrix least-squares procedures on F^2 with SHELXTL (Version 6.14).[31] All non-hydrogen atoms were refined anisotropically. Hydrogen atoms on carbon were included in calculated positions and were refined using a riding model. Hydrogen atoms on nitrogen were located in the difference map and refined semifreely with the help of a distance restraint. PLATON[32] was used to verify all stereochemical configuration designations. ORTEP-3[33] was used to generate Figures 2 and 3. Crystallographic data for the structures reported in this paper are given in the Supporting Information.

Typical Procedure for Synthesis of Dialdehydes. To a flame-dried 250 mL round-bottom flask was added solution of ditosylated ethylene glycol (10 mmol) in freshly distilled acetonitrile (60 mL), followed by the phenol derivative (22 mmol), anhydrous K_2CO_3 (4.14 g, 30 mmol), and NaI (ca. 50 mg). The reaction was stirred at reflux for 12 h, allowed to cool to room temperature, and concentrated under reduced pressure. The resulting residue was partitioned between CH_2Cl_2 (150 mL) and 1 M NaOH (50 mL). The organic phase was washed with an additional portion of 1 M NaOH (50 mL) and saturated brine (50 mL), dried over Na_2SO_4, and concentrated to yield the product, which was of sufficient purity to be used in the subsequent macrocyclization step but could be further purified by column chromatography or recrystallization. Yields refer to material obtained directly after extraction.

*Triethylene Glycol Di(p-formylphenyl) Ether (**9**).* Yellow solid (3.150 g, 88%); R_f (2:1 EtOAc:hexanes): 0.43. ^{1}H NMR (300 MHz, $CDCl_3$): δ 9.86 (s, 1H), 7.79 (d, J = 8.9 Hz, 2H), 6.98 (d, J = 8.9 Hz, 2H), 4.18 (m, 2H), 3.87 (t, J = 4.7 Hz, 2H), 3.74 (s, 2H). ^{13}C NMR (75 MHz, $CDCl_3$): 191.1, 164.0, 132.2, 130.3, 115.1, 71.1, 69.8, 67.9.

*Triethylene Glycol Di(o-formylphenyl) Ether (**13**).* Pale yellow oil (3.364 g, 94%); R_f (1.5:1 EtOAc:hexanes): 0.47. ^{1}H NMR (300 MHz, $CDCl_3$): δ 10.48 (s, 1H), 7.78 (dd, J = 7.7 Hz, J = 1.8 Hz, 1H), 7.52–7.46 (m, 1H), 7.02–6.94 (m, 2H), 4.21 (t, J = 4.7 Hz, 2H), 3.88 (t, J = 4.6 Hz, 2H), 3.72 (s, 2H). ^{13}C NMR (75 MHz, $CDCl_3$): 190.1, 161.4, 136.1, 128.5, 125.3, 121.2, 113.1, 71.2, 69.8, 68.4.

*Diethylene glycol Di(m-formylphenyl) Ether (**14**).* White solid (2.875 g, 93%); R_f (1:1 EtOAc:hexanes): 0.53. ^{1}H NMR (300 MHz, $CDCl_3$): δ 9.94 (s, 1H), 7.44–7.38 (m, 3H), 7.20–7.16 (m, 1H), 4.21 (t, J = 4.7 Hz, 2H), 3.95 (t, J = 4.7 Hz, 2H). ^{13}C NMR (75 MHz, $CDCl_3$): 192.2, 159.5, 138.0, 130.3, 123.9, 122.3, 113.0, 70.0, 67.9.

*Triethylene Glycol Di(m-formylphenyl) Ether (**15**).* Pale yellow solid (3.217 g, 89%); R_f (1.5:1 EtOAc:hexanes): 0.50. ^{1}H NMR (300 MHz, $CDCl_3$): δ 9.91 (s, 1H), 7.42–7.35 (m, 3H), 7.17–7.13 (m, 1H), 4.15 (t, J = 4.7 Hz, 2H), 3.85 (t, J = 4.7 Hz, 2H) 3.72 (s, 2H). ^{13}C NMR (75 MHz, $CDCl_3$): 192.2, 159.5, 137.9, 130.2, 123.8, 122.1, 113.0, 71.1, 69.8, 67.8.

*Tetraethylene Glycol Di(m-formylphenyl) Ether (**16**).* Colorless oil (3.296 g, 82%); R_f (2:1 EtOAc:hexanes): 0.48. ^{1}H NMR (300 MHz, $CDCl_3$): δ 9.93 (s, 1H), 7.44–7.36 (m, 3H), 7.19–7.15 (m, 1H), 4.16 (t, J = 4.8 Hz, 2H), 3.85 (t, J = 4.7 Hz, 2H) 3.73–3.65 (m, 4H). ^{13}C NMR (75 MHz, $CDCl_3$): 192.3, 159.6, 138.0, 130.3, 123.8, 122.3, 113.1, 71.1, 70.1, 69.8, 67.9.

*Diethylene Glycol Di(1-formyl-2-naphthyl) Ether (**17**).* Yellow solid (3.296 g, 82%); R_f (1.5:1 EtOAc:hexanes): 0.53. ^{1}H NMR (300 MHz, $CDCl_3$): δ 10.90 (s, 1H), 9.21 (d, J = 8.7 Hz, 1H), 7.98 (d, J = 9.0 Hz, 1H), 7.72 (bd, J = 7.9 Hz, 1H), 7.60–7.55 (m, 1H), 7.41–7.36 (m, 1H), 7.26–7.23 (m, 1H), 4.39 (t, J = 4.6 Hz, 2H), 3.99 (t, J = 4.6 Hz, 2H). ^{13}C NMR (75 MHz, $CDCl_3$): 192.3, 163.4, 137.7, 131.6, 131.6, 130.0, 129.0, 128.4, 125.2, 117.5, 114.2, 70.3, 69.6.

*Triethylene Glycol Di(1-formyl-2-naphthyl) Ether (**18**).* Yellow solid (4.305 g, 94%); R_f (2:1 EtOAc:hexanes): 0.47. ^{1}H NMR (300 MHz, $CDCl_3$): δ 10.91 (s, 1H), 9.24 (d, J = 8.8 Hz, 1H), 7.98 (d, J = 9.2 Hz, 1H), 7.72 (bd, J = 8.1 Hz, 1H), 7.61–7.56 (m, 1H), 7.42–7.37 (m, 1H), 7.24 (d, J = 9.2 Hz, 1H), 4.35 (t, J = 4.6 Hz, 2H), 3.90 (t, J = 4.6 Hz, 2H), 3.74 (s, 2H). ^{13}C NMR (75 MHz, $CDCl_3$): δ 192.5, 163.7, 137.7, 131.7, 130.0, 128.9, 128.4, 125.2, 125.1, 117.4, 114.3, 71.2, 69.9, 69.5.

Typical Procedure for Synthesis of Macrocycles (*R*,*R*)-1 through (*R*,*R*)-5. To a flame-dried 1 L round-bottom flask was added a solution of (*R*,*R*)-DACH (10.8 mmol, 1.23 g) in anhydrous MeOH (200 mL) and a solution of the dialdehyde (10.8 mmol) in anhydrous MeOH (200 mL). The reaction was stirred at room temperature for 16 h, after which $NaBH_4$ (50 mmol, 1.89 g) was carefully added in small portions over a period of 1 h. The reaction was then brought to reflux for 4 h, concentrated under reduced pressure, and dissolved in a bilayer of CH_2Cl_2 (300 mL) and 1 M NaOH (100 mL). The organic phase was then washed sequentially with an additional portion of 1 M NaOH (100 mL) and brine (100 mL), dried over Na_2SO_4, and concentrated under reduced pressure to give the crude products (typically foamy solids), which were purified by column chromatography on silica gel (~50 cm^3 g^{-1}), using 1–10% NH_3-saturated MeOH:EtOAc as the eluent.

*Tri(ethyleneoxy)-o-phenylene-Linked Macrocycle ((R,R)-**1**).* Colorless oil (2.106 g, 44%); R_f (10% $NH_{3(sat)}$MeOH/EtOAc): 0.56. ^{1}H NMR (300 MHz, $CDCl_3$): δ 7.14–7.04 (m, 2H), 6.84–6.73 (m, 2H), 4.09–4.02 (m, 1H), 3.98–3.92 (m, 2H), 3.77–3.55 (m, 6H), 2.12 (bdd, J = 5.2 Hz, J = 3.2 Hz 1H), 3.46 (d, J = 12.8 Hz, 1H), 2.18–2.10 (m, 2H), 1.89–1.85 (bm, 1H), 1.58–1.54 (bm, 1H), 1.13–1.07 (bm, 1H), 0.98–0.90 (bm, 1H). ^{13}C NMR (75 MHz, $CDCl_3$): δ 157.4, 130.6, 129.9, 128.2, 120.8, 111.7, 71.6, 70.0, 68.4, 62.5, 48.5, 31.7, 25.2. HRMS (ESI, m/z) calcd for $C_{26}H_{37}N_2O_4[M + H]^+$: 441.2748; found: 441.2751.

*Di(ethyleneoxy)-m-phenylene-Linked Macrocycle ((R,R)-**2**).* White foamy solid (2.377 g, 55%); R_f (3% $NH_{3(sat)}$MeOH/EtOAc): 0.39. ^{1}H NMR (300 MHz, $CDCl_3$): δ 7.16 (t, J = 7.9 Hz, 1H), 7.09 (bt, 1H), 6.79–6.73 (m, 2H), 4.14–4.11 (m, 2H), 3.95–3.88 (m, 3H), 3.56 (d, J = 12.8 Hz, 1H), 2.28–2.19 (bm, 2H), 1.84 (bd, J = 8.6 Hz, 1H), 1.28–1.21 (bm, 1H), 1.08–1.01 (bm, 1H). ^{13}C NMR (75 MHz, $CDCl_3$): δ 159.3, 142.7, 129.0, 120.9, 114.6, 112.5, 71.4, 67.5, 61.3, 50.8, 31.6, 25.1. HRMS (ESI, m/z) calcd for $C_{24}H_{33}N_2O_3[M + H]^+$: 397.2486; found: 397.2497.

*Tri(ethyleneoxy)-m-phenylene-Linked Macrocycle ((R,R)-**3**).* White foamy solid (2.880 g, 61%); R_f (3% $NH_{3(sat)}$MeOH/EtOAc): 0.29. ^{1}H NMR (300 MHz, $CDCl_3$): δ 7.15 (t, J = 7.9 Hz, 1H), 6.97 (bt, 1H), 6.80–6.76 (m, 2H), 4.04–4.01 (m, 2H), 3.90–3.82 (m, 3H), 3.72 (s, 2H), 3.58 (d, J = 12.6 Hz, 1H), 2.24–2.16 (bm, 2H), 1.72 (bd, J = 9.8 Hz, 1H), 1.28–1.14 (bm, 1H), 1.06–0.99 (bm, 1H). ^{13}C NMR (75 MHz, $CDCl_3$): δ 159.2, 142.6, 129.1, 120.9, 113.6, 113.0, 70.9, 69.9, 67.3, 60.9, 50.8, 31.5, 25.1. HRMS (ESI, m/z) calcd for $C_{26}H_{37}N_2O_4[M + H]^+$: 441.2748; found: 441.2761.

*Tetra(ethyleneoxy)-m-phenylene-Linked Macrocycle ((R,R)-**4**).* White foamy solid (2.682 g, 57%); R_f (3% $NH_{3(sat)}$MeOH/EtOAc): 0.28. ^{1}H NMR (300 MHz, $CDCl_3$): δ 7.13 (t, J = 7.9 Hz, 1H), 6.88 (bt, 1H), 6.79–6.76 (m, 2H), 4.04–3.77 (m, 5H), 3.66 (s, 4H), 3.55 (d, J = 13.0 Hz, 1H), 2.24–2.163 (bm, 3H), 1.70 (bd, J = 8.4 Hz, 1H), 1.23–1.17 (bm, 1H), 1.07–1.00 (bm, 1H). ^{13}C NMR (75 MHz, $CDCl_3$): δ 159.3, 142.6, 129.2, 120.9, 113.9, 113.3, 71.0, 70.9, 69.8, 67.5 60.9, 50.8, 31.5, 25.2. HRMS (ESI, m/z) calcd for $C_{26}H_{37}N_2O_4[M + H]^+$: 485.3010; found: 485.3018.

*Tri(ethyleneoxy)-p-phenylene-Linked Macrocycle ((R,R)-**5**).* Colorless oil (1.959 g, 41%); R_f (10% $NH_{3(sat)}$MeOH/EtOAc): 0.48. ^{1}H NMR (300 MHz, $CDCl_3$): δ 7.16 (d, J = 8.5 Hz, 2H), 6.81 (d, J = 8.5

Hz, 2H), 4.09 (bt, 2H), 3.84−3.72 (m, 5H), 3.49 (d, J = 12.9 Hz, 1H), 2.26−2.13 (bm, 2H), 1.71 (bd, J = 8.1 Hz, 1H), 1.23−1.18(bm, 1H), 1.07−1.01 (bm, 1H). ^{13}C NMR (75 MHz, $CDCl_3$): δ 157.9, 133.6, 129.3, 114.7, 71.1, 70.1, 67.7, 61.0, 50.4, 31.8, 25.3. HRMS (ESI, m/z) calcd for $C_{26}H_{37}N_2O_4[M + H]^+$: 441.2748; found: 441.2745.

Typical Procedure for Synthesis of Macrocycles (*R*,*R*)-6 and (*R*,*R*)-7. To a flame-dried 1 L round-bottom flask was added a solution of (*R*,*R*)-DACH (4.9 mmol, 0.56 g) in dry CH_2Cl_2 (200 mL) and a solution of the dialdehyde (4.9 mmol) in dry CH_2Cl_2 (200 mL). The reaction was stirred at room temperature for 16 h. After this time, MeOH (100 mL) was added and $NaBH_4$ (28 mmol, 1.06 g) was carefully introduced in small portions over a period of 1 h. The reaction was then refluxed for 4 h, concentrated under reduced pressure, and dissolved in a bilayer of CH_2Cl_2 (300 mL) and 1 M NaOH (100 mL). The organic phase was then washed sequentially with an additional portion of 1 M NaOH (100 mL) and brine (100 mL), dried over Na_2SO_4, and concentrated under reduced pressure to give the crude products (typically foamy solids), which were purified by column chromatography on silica gel (~50 cm^3 g^{-1}), using 1−5% NH_3-saturated MeOH:EtOAc as the eluent.

*Di(ethyleneoxy)-1,2-naphthyl-Linked Macrocycle ((R,R)-**6**).* Yellow oil (0.875 g, 36%); R_f (3% $NH_{3(sat)}$MeOH/EtOAc): 0.23. ^{1}H NMR (300 MHz, $CDCl_3$): δ 8.01 (d, J = 8.8 Hz, 1H), 7.75−7.68 (m, 2H), 7.46−7.40 (m, 1H) 7.32−7.27 (m, 1H) 7.19 (d, J = 8.9 Hz, 1H) 4.33−4.18 (m, 4H) 4.01−3.87 (m, 2H), 2.43−2.41 (bm, 1H), 2.21−2.17 (bm, 1H), 1.68−1.66 (bm, 1H) 1.24−1.10 (bm, 2H). ^{13}C NMR (75 MHz, $CDCl_3$): δ 154.6, 133.5, 129.5, 128.8, 128.6, 126.7, 123.6, 123.4, 123.4, 114.8, 70.2, 69.1, 61.6, 41.3, 32.1, 25.1. HRMS (ESI, m/z) calcd for $C_{32}H_{37}N_2O_3[M + H]^+$: 497.2799; found: 497.2810.

*Tri(ethyleneoxy)-1,2-naphthyl-Linked Macrocycle ((R,R)-**7**).* Yellow foamy solid (1.342 g, 51%); R_f (10% $NH_{3(sat)}$MeOH/EtOAc): 0.58. ^{1}H NMR (300 MHz, $CDCl_3$): δ 7.97 (d, J = 8.5 Hz, 1H), 7.72−7.66 (m, 2H), 7.28−7.23 (m, 1H) 7.18−7.13 (m, 1H) 7.05 (d, J = 8.9 Hz, 1H) 4.45 (d, J = 11.1 Hz, 1H) 4.05 (bt, J = 9.3 Hz, 1H), 3.76 (d, J = 11.1 Hz, 1H), 3.65−3.38 (m, 4H), 3.27−3.22 (m, 1H) 2.37−2.34 (bm, 2H), 1.78 (bd J = 8.6 Hz, 1H), 1.36−1.30 (bm, 1H) 1.21−1.13 (bm, 1H). ^{13}C NMR (75 MHz, $CDCl_3$): δ 154.7, 133.5, 129.4, 128.5, 128.1, 126.5, 124.0, 123.5, 123.2, 115.3, 71.5, 70.5, 69.4, 63.1, 41.9, 32.1, 25.3. HRMS (ESI, m/z) calcd for $C_{34}H_{41}N_2O_3[M + H]^+$: 541.3061; found: 541.3065.

■ ASSOCIATED CONTENT

Supporting Information

Characterization data for macrocyclic compounds, results of molecular modeling, ^{1}H NMR and NOESY studies. This material is available free of charge via the Internet at http://pubs.acs.org.

■ AUTHOR INFORMATION

Corresponding Author

*E-mail: andersef@newpaltz.edu. Fax: (845) 257 3791.

■ ACKNOWLEDGMENTS

We thank Professor Christopher Hunter of the University of Sheffield providing NMRTit HGG. X-ray diffraction facilities were provided by the US National Science Foundation (grants 0521237 and 0911324 to J.M.T.) and Vassar College. Mass spectrometry was performed using instrumentation supported by funding from a National Science Foundation Major Research Instrumentation Grant (#1039659, Teresa A. Garrett, P. I.) Acknowledgement is made to the donors of the American Chemical Society Petroleum Research Fund for support of this research through a New Undergraduate Investigator Award (PRF# 49510-UNI3) to J.F.F.-A. and to the State University of New York at New Paltz for financial support.

■ REFERENCES

(1) (a) Diederich, F. In *Cyclophanes*; Stoddart, J. F., Ed.; Monographs in Supramolecular Chemistry 2; The Royal Society of Chemistry: Cambridge, UK, 1991; pp 222−245. (b) Webb, T. H.; Wilcox, C. S. *Chem. Soc. Rev.* **1993**, *22*, 383−395. (c) Zhang, X. X.; Bradshaw, J. S.; Izatt, R. M. *Chem. Rev.* **1997**, *97*, 3313−3361. (d) Stibor, I.; Zlatuskova, P. *Top. Curr. Chem.* **2005**, *255*, 31−63.

(2) (a) Jadhav, V. D.; Schmidtchen, F. P. *J. Org. Chem.* **2008**, *73*, 1077−1087. (b) Schneider, H.-G. *Angew. Chem., Int. Ed.* **2009**, *48*, 3924−3977. (c) Carrillo, R.; López-Rodríguez, M.; Martín, V. S.; Martín, T. *Angew. Chem., Int. Ed.* **2009**, *48*, 7803−7808. (d) González-Álvarez, A.; Alfonso, I.; Díaz, P.; García-España, E.; Gotor-Fernández, V.; Gotor, V. *J. Org. Chem.* **2008**, *73*, 374−382. (e) Rekharsky, M. V.; Yamamura, H.; Ionue, C.; Kawai, M.; Osaka, I.; Arakawa, R.; Shiba, K.; Sata, A.; Ko, Y. H.; Selvapalam, N.; Kim, K.; Inoue, Y. *J. Am. Chem. Soc.* **2006**, *128*, 14871−14880. (f) Schmuck, C.; Wich, P. *Angew. Chem., Int. Ed.* **2006**, *45*, 4277−4281. (g) Gong, J.; Gibb, B. C. *Chem. Commun.* **2005**, 3319−3321. (h) Rossi, A.; Kyne, G. M.; Turner, D. L.; Wells, N. J.; Kilburn, J. D. *Angew. Chem., Int. Ed.* **2002**, *41*, 4233−4236. (i) Sirikulkajorn, A.; Tuntulani, T.; Ruangpornvistuti, V.; Tomapataget, B.; Davis, A. P. *Tetrahedron* **2010**, *66*, 7423−7428.

(3) (a) Harmata, M. *Acc. Chem. Res.* **2004**, *37*, 862−873. (b) Ema, T.; Tanida, D.; Sugita, K.; Saki, T.; Miyazawa, K.; Ohnishi, A. *Org. Lett.* **2008**, *10*, 2365−2368. (c) Snyder, S. E.; Carey, J. R.; Pirkle, W. H. *Tetrahedron* **2005**, *61*, 7562−7567. (d) Breccia, P.; Van Gool, M.; Pérez-Fernández, R.; Martín-Santamaría, S.; Gago, F.; Prados, P.; de Mendoza, J. *J. Am. Chem. Soc.* **2003**, *125*, 8270−8284. (e) Schuur, B.; Verkuijl, B. J. V.; Minnaard, A. J.; de Vries, J. G.; Heeres, H. J.; Feringa, B. L. *Org. Biomol. Chem.* **2011**, *9*, 36−51. (f) Lewandowski, K.; Murer, P.; Svec, F.; Frechet, J. M. J. *Chem. Commun.* **1998**, 2237−2238. (g) Bunzen, J.; Kiehne, I.; Benkhäuser-Schunk, C.; Lützen, A. *Org. Lett.* **2009**, *11*, 4786−4789.

(4) (a) Pu, L. *Chem. Rev.* **2004**, *104*, 1687−1716. (b) Hembury, G. A.; Borokov, V. V.; Inoue, Y. 2008, *108*, 1−73. (c) Accetta, A.; Corradini, R.; Marchelli, R. *Top. Curr. Chem.* **2011**, *300*, 175−216. (d) Zhu, L.; Zhong, Z.; Anslyn, E. V. *J. Am. Chem. Soc.* **2005**, *127*, 4260−4269. (e) Ema, T.; Tanida, D.; Sakai, T. *J. Am. Chem. Soc.* **2007**, *129*, 10591−10596. (f) Liu, S.; Pestano, J. P. C.; Wolf, C. *J. Org. Chem.* **2008**, *73*, 4267−4270. (g) James, T. D.; Sandanayake, K. R. A. S.; Shinkai, S. *Nature* **1995**, *374*, 345−347. (h) Han, C.; Hou, X.; Zhang, H.; Guo, W.; Li, H.; Jiang, L. *J. Am. Chem. Soc.* **2011**, *133*, 7644−7647. (i) Yu, S.; DeBerarinis, A. M.; Turlington, M.; Pu, L. *J. Org. Chem.* **2011**, *76*, 2814−2819. (j) Reetz, M. T.; Sostmann, S. *Tetrahedron* **2001**, *57*, 2515−2520. (k) Kubo, Y.; Maeda, S.; Tokita, S.; Kubo, M. *Nature* **1996**, *382*, 522−524. (l) Tsubaki, K.; Tanima, D.; Nuruzzaman, M.; Kusumoto, T.; Fuji, K.; Kawabata, T. *J. Org. Chem.* **2005**, *70*, 4609−4616.

(5) (a) Kyba, E. B.; Koga, K.; Sousa, L. R.; Siegel, M. G.; Cram, D. J. *J. Am. Chem. Soc.* **1973**, *95*, 2692−2693. (b) Lehn, J.-M.; Sirlin, C. *J. Chem. Soc., Chem. Commun.* **1978**, 949−951. (c) Petti, M. A.; Shepodd, T. J.; Barrans, R. E. Jr.; Dougherty, D. A. *J. Am. Chem. Soc.* **1988**, *110*, 6825−6840. (d) Echavarren, A.; Galá, A.; Lehn, J.-M.; de Mendoza, J. *J. Am. Chem. Soc.* **1989**, *111*, 4994−4995. (e) Yoon, S. S.; Still, W. C. *J. Am. Chem. Soc.* **1993**, *115*, 823−824. (f) Reetz, M. T.; Huff, J.; Rudolph, J.; Töllner, K.; Deege, A.; Goddard, R. *J. Am. Chem. Soc.* **1994**, *116*, 11588−11589. (g) Pieters, R. J.; Diederich, F. *Chem. Commun.* **1996**, 2255−2256. (h) Asakawa, M.; Brown, C. L.; Pasini, D.; Stoddart, J. F.; Wyatt, P. G. *J. Org. Chem.* **1996**, *61*, 7234−7235. (i) Ogoshi, H.; Mizutani, T. *Acc. Chem. Res.* **1998**, *31*, 81−89. (j) Chin, J.; Lee, S. S.; Lee, K. J.; Park, S.; Kim, D. H. *Nature* **1999**, *401*, 254−257. (k) Rivera, J. M.; Martín, T.; Rebek, J. Jr. *J. Am. Chem. Soc.* **2001**, *123*, 5213−5220. (l) Fiedler, D.; Leung, D. H.; Bergman, R. G.; Raymond, K. N. *J. Am. Chem. Soc.* **2004**, *126*, 3674−3675. (m) Ikeda, T.; Hirata, O.; Takeuchi, M.; Shinkai., S. *J. Am. Chem. Soc.* **2006**, *128*, 16008−16009. (n) Heo, J.; Mirkin, C. A. *Angew. Chem., Int. Ed.* **2006**, *45*, 941−944. (o) Shoji, Y.; Tashiro, K.; Aida, T. *J. Am. Chem. Soc.* **2010**, *132*, 5928−5929.

(6) (a) Fokkens, J.; Klebe, G. *Angew. Chem., Int. Ed.* **2006**, *45*, 985−989. (b) Obst, U.; Betschmann, P.; Lerner, C.; Seiler, P.; Diederich, F.;

Gramlich, V.; Weber, L.; Banner, D. W.; Schönholzer, P. *Helv. Chim. Acta* **2000**, *83*, 855−909.
(7) (a) Miyaji, H.; Hong, S.-H.; Jeong, S.-D.; Yoon, D.-W.; Na, H.-K.; Hong, J.; Ham, S.; Sessler, J. L.; Lee, C.-H. *Angew. Chem., Int. Ed.* **2007**, *46*, 2508−2511. (b) Olivia, A. I.; Simón, L.; Muñiz, F. M.; Sanz, F.; Morán, J. R. *Org. Lett.* **2004**, *7*, 1155−1157. (c) Gavin, J. A.; Garcia, M. E.; Benesi, A. J.; Mallouk, T. E. *J. Org. Chem.* **1998**, *63*, 7663−7669.
(8) (a) Parker, D. *Chem. Rev.* **1991**, *91*, 1441−1457. (b) Wenzel, T. J. *Discrimination of Chiral Compounds Using NMR Spectroscopy*; Wiley: Hoboken, NJ, 2007. (c) Pham, N. H.; Wenzel, T. J. *J. Org. Chem.* **2011**, *76*, 986−989. (d) Yang, D.; Li, X.; Fan, Y.-F.; Zhang, D.-W. *J. Am. Chem. Soc.* **2005**, *127*, 7996−7997. (e) Ma, F.; Al, L.; Shen, X.; Zhang, C. *Org. Lett.* **2007**, *9*, 125−127. (f) Tanaka, K.; Fukuda, N. *Tetrahedron: Asymmetry* **2009**, *20*, 111−114. (g) Moon, L. S.; Pal, M.; Kasetti, Y.; Bharatam, P. V.; Jolly, R. S. *J. Org. Chem.* **2010**, *75*, 5487−5498. (h) Iwaniuk, D. P.; Wolf, C. *J. Org. Chem.* **2010**, *75*, 6724−6727. (i) Chin, J.; Kim, D. C.; Kim, H.-J.; Panosyan, F. B.; Kim, K. M. *Org. Lett.* **2004**, *6*, 2591−2593. (j) Fulwood, R.; Parker, D. *J. Chem. Soc., Perkin Trans. 2* **1994**, 57−64.
(9) (a) Seco, J. M.; Quiñoá, E.; Riguera, R. *Chem. Rev.* **2004**, *104*, 17−177. (b) Fukui, H.; Fukushi, Y. *Org. Lett.* **2010**, *12*, 2856−2859.
(10) (a) Tsukamamoto, M.; Kagan, H. B. *Adv. Synth. Catal.* **2002**, *344*, 453−463. (b) Reetz, M. T. *Angew. Chem., Int. Ed.* **2001**, *40*, 284−310. (c) Nieto, S.; Dragna, J. M.; Anslyn, E. V. *Chem.—Eur. J.* **2010**, *16*, 227. (d) Matsushita, M.; Yoshida, K.; Yamamoto, N.; Wirsching, P.; Lerner, R. A.; Janda, K. D. *Angew. Chem., Int. Ed.* **2003**, *42*, 5984−5987. (e) Abato, P.; Seto, C. T. *J. Am. Chem. Soc.* **2001**, *123*, 9206−9207. (f) van Delden, R. A.; Feringa, B. L. *Angew. Chem., Int. Ed.* **2001**, *40*, 3198−3120.
(11) CSAs that rely on metal coordination are often exceptions. See: (a) Staubach, B.; Buddrus, J. *Angew. Chem., Int. Ed. Engl.* **1996**, *35*, 1344−1346. (b) Kim, H.-J.; Kim, W.; Lough, Kim, B.; Moon, Chin, J. *J. Am. Chem. Soc.* **2005**, *127*, 16776−16777. (c) Kim, W.; So, S. M.; Chagal, L.; Lough, A. J.; Lim, B. M.; Chin, J. *J. Org. Chem.* **2006**, *71*, 8966−8968.
(12) Bennani, Y. L.; Hanessian, S. *Chem. Rev.* **1997**, *97*, 3161−3195.
(13) (a) Nativi, C.; Francesconi, O.; Gabrielli, G.; Vacca, A.; Roelens, S. *Chem.—Eur. J.* **2011**, *17*, 4814−4820. (b) Ryan, K.; Gershell, L. J.; Still, W. C. *Tetrahedron* **2000**, 3309−3318. (c) Amendola, V.; Boiocchi, M.; Estiban-Gómez, D.; Fabbrizzi, L.; Monzani, E. *Org. Biomol. Chem.* **2005**, *3*, 2632−2639.
(14) (a) Taylor, M. S.; Jacobsen, E. N. *Angew. Chem., Int. Ed.* **2006**, *45*, 1520−1543. (b) Trost, B. M.; Miller, J. R.; Hoffman, C. M. *J. Am. Chem. Soc.* **2011**, *133*, 8165−8167. (c) Evans, D. A.; Mito, S.; Seidel, D. *J. Am. Chem. Soc.* **2007**, *129*, 11583−11592. (d) Boga, C.; Fiorelli, C.; Savoia, D. *Synthesis* **2006**, *2*, 285−292.
(15) Folmer-Andersen, J. F.; Lynch, V. M.; Anslyn, E. V. *J. Am. Chem. Soc.* **2005**, *127*, 7986−7987.
(16) (a) Yang, X.; Lui, X.; Shen, K.; Zhu, C.; Cheng, Y. *Org. Lett.* **2011**, *13*, 3510−3513. (b) Li, Z.-B.; Lin, J.; Pu, L. . *Angew. Chem., Int. Ed.* **2005**, *44*, 1690−1693.
(17) (a) Gasparrini, F.; Misiti, D.; Still, W. C.; Villani, C.; Weenmers, H. *J. Org. Chem.* **1997**, *62*, 8221−8224. (b) Reeve, T. B.; Cros, J.-P.; Gennari, C.; Piarulli, U.; de Vries, J. G. *Angew. Chem., Int. Ed.* **2006**, *45*, 2449−2453. (c) Scrimin, P.; Tecilla, P.; Tonellato, U. *Tetrahedron* **1995**, *51*, 217−230. (d) Gawronski, J.; Grycz, P.; Kwit, M.; Rychlewska, U. *Chem.—Eur. J.* **2002**, *8*, 4210−4215.
(18) Sumeier, J. L.; Reilley, C. N. *Anal. Chem.* **1964**, *36*, 1707−1712.
(19) Bertsch, C. R.; Fernelius, W. C.; Block, B. P. *J. Phys. Chem.* **1958**, *62*, 444−450.
(20) (a) Gualandi, A.; Cerisoli, L.; Stoekli-Evans, H.; Savoia, D. *J. Org. Chem.* **2011**, *76*, 3399−3408. (b) Gao, J.; Zingaro, R. A.; Reibenspies, J. H.; Martell, A. E. *Org. Lett.* **2004**, *6*, 2453−2455. (c) Li., Z.-B.; Lin, J.; Sabat, M.; Hyacinth, M.; Pu, L. *J. Org. Chem.* **2007**, *72*, 4905−4916. (d) Hodacová, J.; Chadim, M.; Závada, J.; Aguilar, J.; García-España, E.; Luis, S. V.; Miravet, J. F. *J. Org. Chem.* **2005**, *70*, 2042−2047. (e) Gawronski, J.; Brzostowska, M.; Kwit, M.; Plutecka, A.; Pychlewska, U. *J. Org. Chem.* **2005**, *70*, 10147−10150. (f) Padmaja, M.; Periasamy, M. *Tetrahedron: Asymmetry* **2004**, *15*, 2437−2441.
(21) Correa, W. H.; Scott, J. L. *Molecules* **2004**, *9*, 513−519.
(22) (a) Dvornikovs, V.; Smithrud, D. B. *J. Org. Chem.* **2002**, *67*, 2160−2167. (b) Murahashi, S.-I.; Noji, S.; Komiya, N. *Adv. Synth. Catal.* **2004**, *346*, 195−198.
(23) See Supporting Information for details of molecular modeling studies.
(24) (a) Busto, E.; González-Álvarez, A.; Gotor-Fernández, V.; Alfonso, I.; Gotor, V. *Tetrahedron* **2010**, *66*, 6070−6077. (b) Demirtas, H. N.; Bozkurt, S. B.; Durmaz, M.; Yilmaz, M.; Sirit, A. *Tetrahedron: Asymmetry* **2008**, *19*, 2020−2025. (c) Altava, B.; Burgete, M. I.; Carbó, N.; Escorihuela, J.; Luis, S. V. *Tetrahedron: Asymmetry* **2010**, *21*, 982−989. (d) Wu, Y.; Guo, H.; James, T. D.; Jhao, J. *J. Org. Chem.* **2011**, *76*, 5685−5695. (e) He, X.; Zhang, Q.; Wang, W.; Lin, L.; Liu, X.; Feng, X. *Org. Lett.* **2011**, *13*, 804−807. (f) Zheng, Y.-S.; Zhang, C. *Org. Lett.* **2004**, *13*, 1189−1192.
(25) Connors, K. A. *Binding Constants, The Measurement of Molecular Complex Stability*; Wiley-Interscience: New York, 1987; pp 147−149.
(26) Bisson, A. P.; Hunter, C. A.; Morales, J. C.; Young, K. *Chem.—Eur. J.* **1998**, *4*, 845−851.
(27) Fielding, L. *Tetrahedron* **2000**, *56*, 6151−6170.
(28) Schanz, H.-J.; Linseis, M. A.; Gilheany, D. G. *Tetrahedron: Asymmetry* **2003**, *14*, 2763−2769.
(29) Bonger, K. M.; van den Berg, R. J. B. H. N.; Heitman, L. H.; IJzerman, A. P.; Oosterom, J.; Timmers, C. M.; Overkleeft, H. S.; van der Marel, G. A. *Bioorg. Med. Chem. Lett.* **2007**, *15*, 4841−4856.
(30) Connors, K. A. *Binding Constants, The Measurement of Molecular Complex Stability*; Wiley-Interscience: New York, 1987; pp 21−24.
(31) Sheldrick, G. M. *Acta Crystallogr.* **2008**, *A64*, 112−122.
(32) Spek, A. L. *Acta Crystallogr.* **2009**, *D65*, 148−155.
(33) Farrugia, L. J. *J. Appl. Crystallogr.* **1997**, *30*, 565.